considération que ses seuls sous-groupes invariants et les RIP qui leur sont associées.

Exemple

La Fig. 4 donne le treillis modulaire des sous-groupes invariants du groupe $G=\bar{4}2m$; il est isomorphe du treillis modulaire des RIP associées à ces sous-groupes invariants.

V. Remarques finales

Les propriétés des RIP ont été illustrées dans le présent mémoire sur les exemples des groupes ponctuels $\bar{4}2m$, 23 et $4/m$ qui sont de complexité moyenne. Nous tenons à la disposition du lecteur des tables concernant les 32 groupes ponctuels cristallographiques, les 58 groupes ponctuels bicolores vrais (cristallographiques), les 32 groupes ponctuels bicolores gris (cristallographiques) (Belguith & Billiet, 1989) et des groupes ponctuels non cristallographiques (Masmoudi & Billiet, 1988).

Un domaine d'application des RIP est l'étude des représentations sous-tendues par les vecteurs de liaison des molécules à atome central. C'est le cas, par exemple, de la molécule PCl_5 bipyramidale à base triangulaire dans l'état vapeur qui est caractérisée par le groupe ponctuel $\bar{6}m2$. En voici les positions [notations dérivées directement de celles du groupe d'espace $P\bar{6}m2$ - N° 187 (*International Tables for Crystallography*, 1987)]:

Cl 3 *j* *mm*2 $x, \bar{x}, 0; x, 2x, 0; 2\bar{x}, \bar{x}, 0.$

Cl 2 *g* 3*m*. $0, 0, z; 0, 0, \bar{z};$

P 1 *a* $\bar{6}m2$ $0, 0, 0.$

Les cinq liaisons P-Cl sous-tendent la représentation de permutation $\Gamma=2A_1'+A_2''+E'$ du groupe $\bar{6}m2$. Γ est la somme de deux RIP de ce groupe: $R(3m)=A_1'+A_2''$ sous-tendue par les deux liaisons axiales [2,11 Å; *cf.* Durrant & Durrant (1972)] et $R(mm2)=A_1'+E'$ sous-tendue par les trois liaisons équatoriales [2,04 Å; *cf.* Durrant & Durrant (1972)].

Les RIP d'un groupe sont un cas particulier d'une catégorie plus vaste de représentations induites dites 'monomiales', c'est-à-dire, induites par les représentations monodimensionnelles des sous-groupes (Gorenstein, 1968). Des représentations monomiales plus complexes que les RIP apparaissent lorsqu'on étudie par exemple les représentations sous-tendues par des vecteurs équivalents joignant des positions prises dans deux familles de positions équivalentes d'un groupe ponctuel (molécule à liaisons non centrales) (Masmoudi & Billiet, 1989).

Références

BELGUITH, J. & BILLIET, Y. (1988). *Acta Cryst.* A**44**, 124-127.

BERGER, M. (1977). *Géométrie.* Tome 1. *Action de Groupes, Espaces Affines et Projectifs.* Paris: Cedic/Nathan.

BERTAUT, E. F. (1968). *Acta Cryst.* A**24**, 217-231.

BERTAUT, E. F. (1981). *C. R. Acad. Sci.* **293**, 253-256.

DUBREIL, P. (1963). *Algèbre.* Paris: Gauthier-Villars.

DUBREIL, P. (1972). *Théorie des Groupes.* Paris: Dunod.

DURRANT, P. J. & DURRANT, B. (1972). *Introduction to Advanced Inorganic Chemistry.* Londres: Longman.

GORENSTEIN, D. (1968). *Finite Groups.* New York: Harper & Row.

International Tables for Crystallography (1987). Tome A. Dordrecht: Reidel. (Distributeur actuel Kluwer Academic Publishers, Dordrecht.)

KIRILLOV, A. A. (1976). *Elements of the Theory of Representations.* Berlin: Springer-Verlag.

KUROSH, A. G. (1960). *The Theory of Groups*, Tome 2. New York: Chelsea Publishing Company.

KUROSH, A. G. (1965). *Lectures in General Algebra.* Oxford: Pergamon.

LOMONT, J. S. (1959). *Applications of Finite Groups.* New York: Academic Press.

MASMOUDI, K. & BILLIET, Y. (1989). À paraître.

MURNAGHAM, F. D. (1963). *The Theory of Group Representations.* New York: Dover.

Acta Cryst. (1989). A**45**, 34-39

Bounding a Molecule in a Noisy Synthesis

BY A. G. URZHUMTSEV, V. YU LUNIN AND T. B. LUZYANINA

Research Computer Centre, Academy of Sciences of the USSR, Pushchino, Moscow Region, 142292, *USSR*

(*Received* 2 *February* 1988; *accepted* 14 *July* 1988)

Abstract

A method of bounding a protein molecule in a very noisy synthesis is considered. It consists of two steps. In the first step ('nonlinear filtration') basic points are chosen that are most likely to belong to the region of the molecule. In the second step ('linear filtration') a compact region with the maximal concentration of these points is searched. Various modifications of the method are analysed. It is shown that the molecular

0108-7673/89/010034-06$03.00

region in a finite-resolution synthesis contains not only the highest positive maxima of the density distribution but also the deepest negative minima.

1. Introduction

In the early stages of an X-ray study a situation may arise when an electron density synthesis produced is so noisy that it hardly even allows identification of the contour and the location of the protein molecule. In this paper mathematical techniques are shown which may be used to bound the molecule in such a noisy synthesis. The information obtained may further serve to refine structure-factor phases (Bricogne, 1976; Wang, 1985). The method we use is based on two assumptions:

(i) The electron density synthesis is an accurate representation of the protein molecule (a 'signal') with a superposed random noise. It is also assumed that the noise is not so large as to suppress the signal completely but may be enough to complicate visual identification of the molecule (Fig. 1*b*).

(ii) The protein molecule is a globule, *i.e.* it occupies a compact region in the crystal cell, surrounded by a solvent with the electron density much lower than in the protein.

The method consists of two steps utilizing assumptions (i) and (ii), respectively (Urzhumtsev, 1985). In the first step we choose 'basic points' in the unit cell; these are points which with certainty can be ascribed to the region of the molecule which is searched. Here the simplest way is to take points with relatively high values of electron density $\rho \geq \rho_{\text{crit}}$, exceeding the value of noise. This step is examined more thoroughly in § 2.

In the second step we try to bound a compact region in a cell in which the concentration of basic points is maximal. We consecutively examine all the points $\mathbf{r}$ in the cell and calculate the number $b(\mathbf{r})$ of the basic points which fall in a sphere of radius R with $\mathbf{r}$ as the centre. The largest number of these points corresponds to the centre of the sphere locating inside the boundary of the molecule, and the least to the sphere locating inside the solvent region. A more detailed description of this step and of its effective computer implementation is given in § 3. It should be noted that the concentration function $b(\mathbf{r})$ should not be considered as 'improved' synthesis. The only aim of the $b(\mathbf{r})$ calculation is to produce the 'mask' of the molecular region.

Fig. 1(*c*) shows the result of application of our method to the synthesis of Fig. 1(*b*). The formal procedure is as follows.

$$\rho^m(\mathbf{r}) = \begin{cases} 0 & \text{for } \rho(\mathbf{r}) < \rho_{\text{crit}} \\ 1 & \text{for } \rho(\mathbf{r}) \geq \rho_{\text{crit}}. \end{cases} \quad (1)$$

$$b(\mathbf{r}) = C \int_{|\mathbf{r}-\mathbf{u}| \leq R} \rho^m(\mathbf{u})\, \mathrm{d}V_{\mathbf{u}}. \quad (2)$$

A close approach to bounding a molecule has been proposed by Wang (1985). It also breaks into two essential steps. The first is the transform of the initial synthesis,

$$\rho^m(\mathbf{r}) = \begin{cases} 0 & \text{for } \rho(\mathbf{r}) \leq F_{000}/V \\ \rho(\mathbf{r}) - F_{000}/V & \text{for } \rho(\mathbf{r}) > F_{000}/V. \end{cases} \quad (3)$$

(In practice this transform is done by calculating the synthesis without F_{000} and zeroing it at the points with negative values.) In the second step, for every point $\mathbf{r}$ in the unit cell the weighted mean of the modified electron density is calculated in a sphere of radius R with $\mathbf{r}$ as the centre:

$$b^W(\mathbf{r}) = C \int_{|\mathbf{r}-\mathbf{u}| \leq R} (R - |\mathbf{r}-\mathbf{u}|)\rho^m(\mathbf{u})\, \mathrm{d}V_{\mathbf{u}}. \quad (4)$$

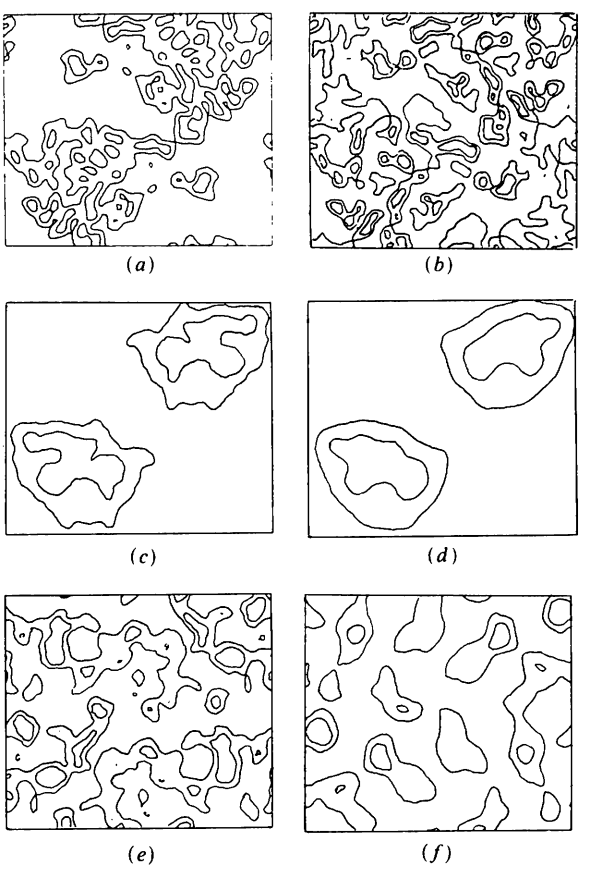

Fig. 1. Section $z = 12/48$. Contours $\rho(\mathbf{r}) = \rho_i^0$ $(i = 1, 2)$ are presented where ρ_i^0 for each of the syntheses are chosen so that the points with $\rho(\mathbf{r}) \geq \rho_i^0$ $(i = 1, 2)$ occupy 40 and 10% of the volume of the unit cell. (*a*) Synthesis $\rho_{ex}(\mathbf{r})$ constructed over the full 4 Å set of exact structure factors; (*b*) synthesis $\rho_n(\mathbf{r})$ with 18% of reflections excluded from $\rho_{ex}(\mathbf{r})$; (*c*) synthesis $\rho_n(\mathbf{r})$ after the treatment (1)-(2) ($\rho_{\text{crit}} = 0{\cdot}40$ e Å^{-3}, $R = 10$ Å); (*d*) synthesis $\rho_n(\mathbf{r})$ after the treatment (3)-(4) ($R = 10$ Å); (*e*) synthesis $\rho_n(\mathbf{r})$ averaged by (2) ($R = 10$ Å); (*f*) synthesis $\rho_n(\mathbf{r})$ averaged with the weight (4) ($R = 10$ Å).

Fig. 1(*d*) shows the result of application of Wang's (1985) method to the synthesis of Fig. 1(*b*).

More detailed comparison of the methods (1)-(2) and (3)-(4) is made at the end of the paper.

2. Nonlinear filtration

2.1. *Necessity of nonlinear filtration*

Before we discuss in detail the first step of the synthesis treatment, we want to show that generally this step cannot be neglected, otherwise the transforms (2) or (4) applied directly to the initial synthesis will not allow bounding of the molecule of interest (Figs. 1*e*, *f*).

The test object was a subtilisin model placed into a 73·0 × 64·0 × 48 Å unit cell in space group $P2_12_12_1$. The centre of the molecule was chosen so that different symmetry-bound molecules did not overlap. The atomic coordinates were used to calculate structure factors $F_{ex}(\mathbf{s})\exp[i\varphi_{ex}(\mathbf{s})]$, and an 'exact' synthesis $\rho_{ex}(\mathbf{r})$ with a resolution of 4 Å was obtained. This synthesis was used for the checking of results only. One of its sections is shown in Fig. 1(*a*).

In general, the synthesis is noisy if (i) it is calculated from erroneous structure factor phases; and (ii) the calculation does not include the terms corresponding to structure factors for which either modules are not found experimentally or phases are lacking.

To simulate a noisy synthesis, we excluded 18% of terms from the calculation of the exact synthesis $\rho_{ex}(\mathbf{r})$ and took absolutely accurate phases for the remaining reflections. A section of the synthesis $\rho_n(\mathbf{r})$ obtained is shown in Fig. 1(*b*). Let us stress that all the deformations in the synthesis of Fig. 1(*b*) are the result of merely excluding some reflections. The phases of those retained were quite correct. Mainly excluded were reflections in the central area around the axis 1. These are reflections which on technical grounds are lost in a real X-ray experiment.

Figs. 1(*e*) and (*f*) illustrate the syntheses $\rho_n(\mathbf{r})$ averaged either directly by (2) or with Wang's weight function by (4). As one can see, here the compact region is not bounded, in contrast with Figs. 1(*c*) and (*d*) which show the result of an averaging after the nonlinear modifications (1) or (3) have been applied.

2.2. *Nonlinear modification of electron density*

There is an extensive literature on the 'modification of electron density' used to improve the quality of syntheses (*e.g.* Qurashi, 1953; Hoppe & Gassmann, 1968; Zwick, Bantz & Hughes, 1976; Simonov, 1976; Vainshtein & Khachaturyan, 1977; Schevitz, Podjarny, Zwick, Hughes & Sigler, 1981; Cannillo, Oberti & Ungaretti, 1983). These authors suggested different approaches to substantiating the modifications they employed. In this section we consider the modification directing the search for basic points.

Two ways of introducing these points to bound a molecule are possible. First, one may unambiguously decide whether a point belongs to the region of the molecule or not. This means the modified function $\rho^m(\mathbf{r})$ will take one of two discrete values (0 or 1). The simplest example of such a modification is the transform (1). The other way is to introduce for every point in the unit cell a weight which could serve as a measure of our certainty that this point belongs to the region of the molecule. Here a good example is the calculation of the probability for every point that this point belongs to the chosen molecule (Urzhumtsev, Lunin & Luzyanina, 1986).

The simplest way of deciding whether every point **r** belongs to a molecule or not is to compare the value of electron density at this point with a threshold ρ_{crit}, *i.e.* perform the transform (1). Here it is clear that if ρ_{crit} is lower than the noise, then the basic points may include a considerable number of points which do not belong to the molecule, thereby preventing the molecule from being bounded properly. Fig. 2 shows the synthesis $\rho_n(\mathbf{r})$ after the transforms (1)-(2) with various threshold values of ρ_{crit}. It can be seen that for a sufficiently high threshold the molecule can be bounded (Fig. 2*a*), and for a lower level the picture is destroyed (Figs. 2*b*, *c*). A non-trivial situation arises when the threshold decreases further (Fig. 2*d*). The concentration of basic points becomes maximal in the solvent, and minimal in the molecule. Below we shall explain this phenomenon.

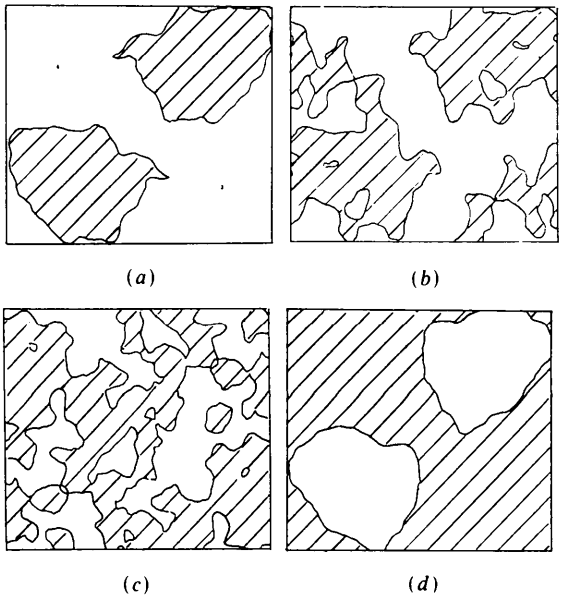

Fig. 2. Synthesis $\rho_n(\mathbf{r})$ after the treatment (1)-(2) with different thresholds ρ_{crit} [in all figures the parameter of (2) is $R = 10$ Å]; shaded is the region $b(\mathbf{r}) \geq b^0$ which constitutes 50% of the cell volume: (*a*) $\rho_{crit} = 0{\cdot}45$; (*b*) $\rho_{crit} = 0{\cdot}28$; (*c*) $\rho_{crit} = 0{\cdot}22$; (*d*) $\rho_{crit} = 0{\cdot}05$.

2.3. *'Negative' image of the molecule*

When a finite-resolution synthesis is calculated, the effect of truncating the Fourier series is observed. It results in more flat peaks and negative values in the synthesis (even if the calculated structure-factor moduli and phases are absolutely accurate). Moreover, the deepest negative minima appear in the synthesis near the highest maxima. Correspondingly, the region of the molecule will contain not only the highest positive maxima but also the deepest negative minima. If the threshold ρ_{crit} in (1) falls below the minimal value in the solvent, then all points in the solvent region will be basic. At the same time all the points which are not basic (deepest negative minima) will remain inside the molecule, thus giving the minimum of (2) within the boundary of the molecule.

The above considerations are confirmed by the following test. As mentioned in § 2.1, we calculated the 'exact' synthesis $\rho_{\text{ex}}(\mathbf{r})$ at a resolution of 4 Å. The minimum and maximum values were −0·45 and 2·42 e Å^{-3}, respectively, and the mean value was $F_{000}/V = 0{\cdot}25$ e Å^{-3}. The solid line in Fig. 3 shows the distribution of frequencies for different values which the electron density takes on in the synthesis $\rho_{\text{ex}}(\mathbf{r})$. Also in this figure the distribution of the frequencies is given separately for the molecule and the solvent regions. The minimum, maximum and mean values for the molecule region were −0·45, 2·42 and 0·29 and for the solvent −0·19, 0·33 and 0·06. The mean square deviation from the mean value in the solvent was $\sigma_{\text{sol}} = 0{\cdot}065$. The region of the molecule was defined in this calculation as the conjunction of the spheres of radii 5 Å for all the atoms in the molecule, with centres at the atomic centres. It occupied 81% of the volume of the unit cell.

It is seen in Fig. 3 that the negative values with the largest moduli are actually concentrated within the molecule.

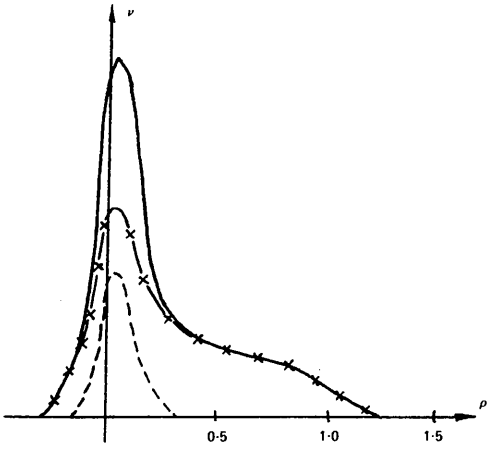

Fig. 3. Histograms for the values $\rho_{\text{ex}}(\mathbf{r})$: in the whole unit cell (——); in the molecular region (×-×-×); in the solvent region (- - -). Here $\nu(\rho)\Delta\rho$ is the portion of the unit cell with the values of $\rho(\mathbf{r})$ within the interval $(\rho, \rho+\Delta\rho)$.

We did not simulate the solvent in the intermolecular region during the test. Therefore, in biological crystals the mean value of $\bar{\rho}_{\text{sol}}$ in the solvent is somewhat higher than in the test.

The property of the molecule to include the points of deepest minima may serve to define its boundaries: the points of extremely small values of $\rho_n(\mathbf{r})$ may also be used as basic. For example, we can use as the first transform the next one:

$$\rho^m(\mathbf{r}) = \begin{cases} 1 & \text{for } \rho(\mathbf{r}) \geq \rho_{\text{crit}}^{\max} \\ 0 & \text{for } \rho_{\text{crit}}^{\min} < \rho(\mathbf{r}) < \rho_{\text{crit}}^{\max} \\ 1 & \text{for } \rho(\mathbf{r}) \leq \rho_{\text{crit}}^{\min}. \end{cases} \tag{5}$$

Values $\bar{\rho}_{\text{sol}} + \sigma_{\text{sol}} + \sigma_n$ and $\bar{\rho}_{\text{sol}} - \sigma_{\text{sol}} - \sigma_n$ may serve the approximate standard thresholds $\rho_{\text{crit}}^{\max}$ and $\rho_{\text{crit}}^{\min}$, respectively. Here $\bar{\rho}_{\text{sol}}$ is the mean value, and σ_{sol} is the mean square deviation for the synthesis $\rho_{\text{ex}}(\mathbf{r})$ in the solvent region. The estimate for the mean square value σ_n of the 'noisy' component of the synthesis may be obtained in the following way (Blundell & Johnson, 1976):

$$\sigma_n^2 = (1/V^2) \sum_{\mathbf{s}} F^2(\mathbf{s})[1 - m^2(\mathbf{s})],$$

where $m(\mathbf{s})$ is the figure of merit in the determination of the structure-factor phases.

For the test in § 2.1 $\sigma_n = 0{\cdot}17$, *i.e.* $\rho_{\text{crit}}^{\max} = 0{\cdot}295$, $\rho_{\text{crit}}^{\min} = -0{\cdot}175$.

3. Linear filtration

The second step in bounding the molecule is the transform (2) or (4) of the modified function $\rho^m(\mathbf{r})$. These transforms can easily be written in a general form as

$$b(\mathbf{r}) = \int_{R^3} a(|\mathbf{r}-\mathbf{u}|)\rho^m(\mathbf{u})\, \mathrm{d}V_{\mathbf{u}} = a * \rho, \tag{6}$$

where * means convolution.

Here, for (2)

$$a(t) = \begin{cases} 3/(4\pi R^3) & \text{for } t \leq R \\ 0 & \text{for } t > R \end{cases} \tag{7}$$

and for (4)

$$a(t) = \begin{cases} (3/\pi R^4)(R-t) & \text{for } t \leq R \\ 0 & \text{for } t > R \end{cases} \tag{8}$$

[the coefficients are given by the normalization condition $\int_{R^3} a(|\mathbf{u}|)\, \mathrm{d}V_{\mathbf{u}} = 1$]. Using the property of the Fourier transform to convert the convolution of functions into the product of their Fourier coefficients, we suggest the following way of calculating (2) (Urzhumtsev, 1985) and (4) (Leslie, 1987): one determines structure factors $F^m(\mathbf{s}) \exp[i\varphi^m(\mathbf{s})]$ of the function $\rho^m(\mathbf{r})$ and finds the function

$$b(\mathbf{r}) = (1/V) \sum_{\mathbf{s}} \tau(\mathbf{s}) F^m(\mathbf{s}) \exp[i\varphi^m(\mathbf{s})], \tag{9}$$

in which the smoothing function $\tau(\mathbf{s})$ is the sinus-Fourier transform of the convolution kernel in (6),

$$\tau(s) = (2/s) \int_0^\infty ta(t) \sin(2\pi st)\, dt.$$

For functions of the forms (6) and (7) the corresponding smoothing functions $\tau(s)$ and $\tau^W(s)$ can easily be defined analytically. For (6)

$$\tau(s) = 3\,\frac{\sin(2\pi sR) - 2\pi sR\cos(\pi sR)}{(2\pi sR)^3},$$

and for (7)

$$\tau^W(s) = 12\,\frac{2[1-\cos(2\pi sR)] - 2\pi sR\sin(2\pi sR)}{(2\pi sR)^4}.$$

These functions are plotted in Fig. 4.

We have used the transform (2) primarily to calculate the number of basic points inside a sphere with the centre moving over the unit cell. Equation (9) gives an opportunity to regard it as a common way of filtering the high-frequency noise. It implies the suppression of the high-frequency components by multiplying them by the function $\tau(s)$ decaying with increasing s (Shevyrev & Simonov, 1981). It is reasonable to suggest that the noise in (9) may be filtered by other functions decreasing with increasing s. An example is (Namba & Stubbs, 1985)

$$\tau^G(s) = \exp[-(2\pi sR)^2/6].$$

This expression corresponds to (6) with the Gaussian

$$a(t) = (3/2\pi R^2)^{3/2} \exp[-(3/2R^2)t^2] \qquad (10)$$

(or, which is the same thing, to averaging with the Gaussian weight function). Fig. 5 shows the result of treatment (1) and (6) of the synthesis $\rho_n(\mathbf{r})$ (Fig. 1*b*) with functions $a(t)$ of the forms (7), (8) and (10). Here we see no principal difference in using some modification or other of $a(t)$. Nevertheless, the result may be slightly better if we use the Gaussian $a(t)$ of the form (9) so that the weight function $\tau^G(s)$ is non-oscillating.

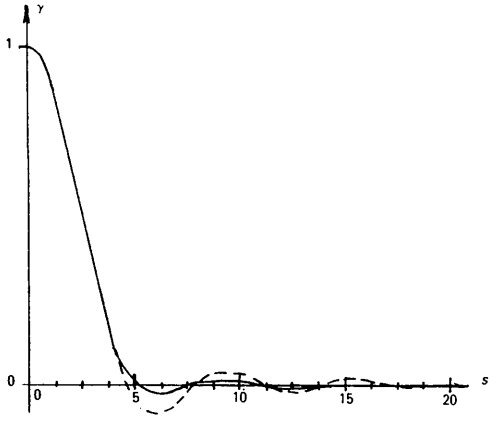

Fig. 4. Smoothing functions in (9): (- - -) for the averaging (2); (——) for the weighted averaging (4).

4. Treatment of syntheses with extremely high noise

The modification (3) of Wang (1985) is independent of the noise in the synthesis treated. On the one hand, this facilitates the work, making estimation of the parameters of the noise component unnecessary. On the other hand, a situation may arise when for a high level of noise a molecule cannot be bounded by (3)-(4), whereas use of (1)-(2) or (5)-(2) with a high level of ρ_{crit} (exceeding the value of noise) will solve this problem. This statement may be illustrated by the following test. The test object was the synthesis

$$\rho_n(\mathbf{r}) = (1/V) \sum_{\mathbf{s}\in S'} F_{\text{ex}}(\mathbf{s})^{\frac{1}{2}} (\exp\{i[\varphi_{\text{ex}}(\mathbf{s}) + \delta(\mathbf{s})]\} + \exp i\varphi_r(\mathbf{s})) \exp[-2\pi i(\mathbf{s}.\mathbf{r})], \qquad (11)$$

where $F_{\text{ex}} \exp(i\varphi_{\text{ex}})$ are structure factors calculated, as above, from the subtilisin model; δ are random normally distributed values with zero means and mean square deviations of 30°; φ_r are phases generated by a randomizer; the set S' includes the same 82% of reflections as before. This level of noise pertains to a synthesis constructed from the incomplete set of reflections with 'best' phases determined with respect to a single heavy-atom derivative. The errors δ imitate the errors caused by inaccurate determina-

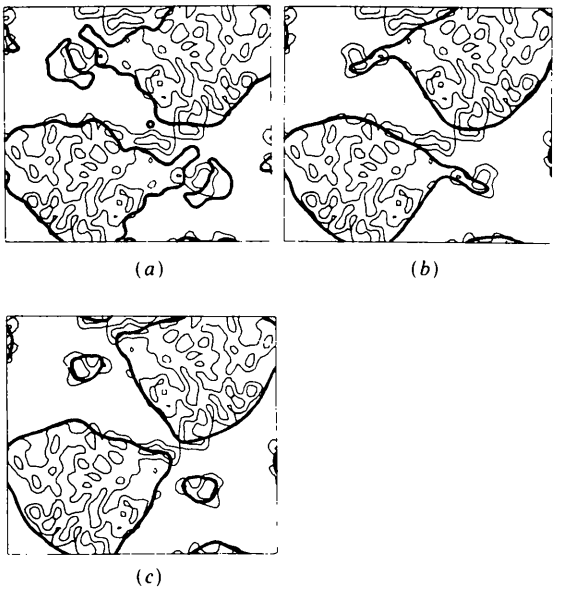

Fig. 5. Boundaries obtained after the treatment (1) and (6) (ρ_{crit} = 0·40, R = 10 Å) with various weighting schemes in (6). The thick line represents the mask produced by the function $b(\mathbf{r})$ which constitutes 60% of the cell volume. The thin line represents the exact synthesis $\rho_{\text{ex}}(\mathbf{r})$ (it bounds 40% of the cell): (*a*) weight function (7); (*b*) weight function (8); (*c*) weight function (10).

tion of heavy-atom parameters. Fig. 6 depicts the synthesis $\rho_n(\mathbf{r})$ before and after the treatments (3)-(4) and (5)-(2).

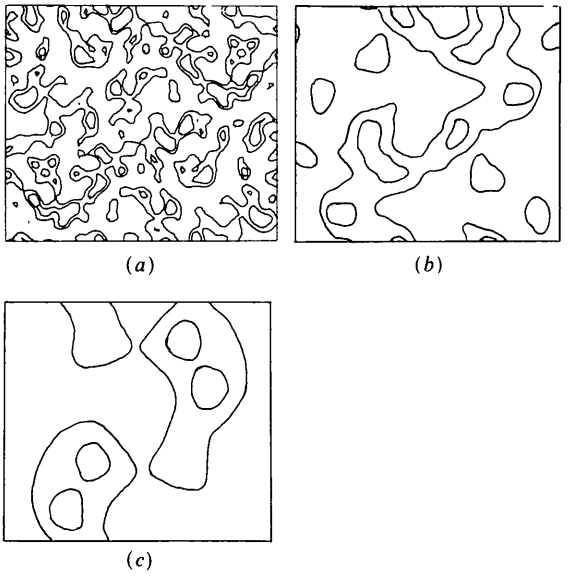

Fig. 6. Section $z = 12/48$: (*a*) the synthesis (11); (*b*) the synthesis (11) after treatment (3)-(4) ($R = 10$ Å); (*c*) the synthesis (11) after treatment (5) and (2) ($\rho_{crit}^{max} = 0{\cdot}56$, $\rho_{crit}^{min} = -0{\cdot}047$, $R = 10$ Å). Bounded is the region $b(\mathbf{r}) > b^0$ which constitutes 40% of the cell volume.

The authors thank O. M. Liginchenko for her help in preparing the manuscript.

References

BLUNDELL, T. L. & JOHNSON, L. N. (1976). *Protein Crystallography.* New York: Academic Press.

BRICOGNE, G. (1976). *Acta Cryst.* A**32**, 823-847.

CANNILLO, E., OBERTI, R. & UNGARETTI, L. (1983). *Acta Cryst.* A**39**, 68-74.

HOPPE, W. & GASSMANN, J. (1968). *Acta Cryst.* B**24**, 97-107.

LESLIE, A. G. V. (1987). *Acta Cryst.* A**43**, 134-136.

NAMBA, K. & STUBBS, G. (1985). *Acta Cryst.* A**41**, 252-262.

QURASHI, M. M. (1953). *Acta Cryst.* **6**, 103.

SCHEVITZ, R. W., PODJARNY, A. D., ZWICK, M., HUGHES, J. J. & SIGLER, P. B. (1981). *Acta Cryst.* A**37**, 669-667.

SHEVYREV, A. A. & SIMONOV, V. I. (1981). *Kristallografiya*, **26**, 36-41.

SIMONOV, V. I. (1976). In *Crystallographic Computing Techniques*, edited by F. R. AHMED, K. HUML & B. SEDLÁČEK, pp. 138-143. Copenhagen: Munksgaard.

URZHUMTSEV, A. G. (1985). *The Use of Local Averaging to Analyse Macromolecular Images in the Electron Density Maps.* Preprint, USSR Academy of Sciences, Pushchino.

URZHUMTSEV, A. G., LUNIN, V. YU. & LUZYANINA, T. B. (1986). Tenth Eur. Crystallogr. Meet., Wrocław, Poland. Coll. Abstracts, pp. 51-52.

VAINSHTEIN, B. K. & KHACHATURYAN, A. G. (1977). *Kristallografiya*, **22**, 706-710.

WANG, B. C. (1985). *Methods Enzymol.* **115**, 90-112.

ZWICK, M., BANTZ, D. & HUGHES, J. (1976). *Ultramicroscopy*, **1**, 275-277.

Acta Cryst. (1989). A**45**, 39-42

Polarization Anisotropy of Anomalous Scattering in Lithium Iodate and Effect of *K*-Level Width

BY DAVID H. TEMPLETON AND LIESELOTTE K. TEMPLETON

Department of Chemistry, University of California, Berkeley, CA 94720, *USA*

(*Received* 23 *March* 1988; *accepted* 18 *July* 1988)

Abstract

The anomalous scattering tensor, measured using synchrotron radiation with lithium iodate near the iodine *K* absorption edge, shows polarization anisotropy similar to that in the bromate ion, but lesser in magnitude: about 1 electron/atom at most. The reduction is explained by a greater natural width of the *K* level. Equally small or smaller anisotropy is predicted for any other absorption edge above 33 keV.

1. Introduction

X-ray dichroism occurs in some molecules near absorption edges as a result of transitions to electronic states which have symmetry that reflects the directional character of the chemical bonding. The anomalous scattering also depends on the direction of polarization of the radiation and needs to be represented by a tensor rather than a scalar function. Having found large effects of this kind for the pyramidal bromate ion near the *K* edge of bromine (Templeton & Templeton, 1985*a*) we were eager to test them in the iodate ion, which has analogous electronic structure and the same pyramidal shape. Lithium iodate, which crystallizes with two molecules per cell in the non-centrosymmetric space group $P6_3$ (Rosenzweig & Morosin, 1966; de Boer, van Bolhuis, Olthof-Hazekamp & Vos, 1966), is a suitable material for observation of the dichroism because the threefold axes of all the iodate ions are parallel. This molecular orientation and the lack of a center of inversion permit

0108-7673/89/010039-04$03.00